Grading of Brain Tumors in Children: Comparative Study between Using Diffusion-Weighted Imaging and 1H-MR Spectroscopy

MAHMOUD M.A. REZK, M.D., Ph.D.*; AYDA A. YOUSEF, M.D., Ph.D.**; DALIA I. MOHAMED, M.D., Ph.D.**; MANAL M. REFAAT BESHIR, M.D., Ph.D.* and MOHSEN AHMED ABDELMOHSEN, M.D., Ph.D.*,***

The Department of Radio-Diagnosis, National Cancer Institute, Cairo University*, Department of Radio-Diagnosis, Faculties of Medicine, Cairo** and Alexandria*, *** Universities

Abstract

Background: Accurate initial diagnosis and grading of the brain tumors is highly affecting choice of treatment, long-term prognosis, and quality of life in survivors. Conventional MRI has a limited accuracy in the tumor grading; that role is reserved for histopathologic evaluation after biopsy. Diffusion weighted image (DWI) and MR spectroscopy (MRS) are used as a non-invasive imaging tools for tumor grading. Thus, the purpose of our study was to compare the effectiveness of both techniques.

Aim of Study: The aim of our study was to answer a question that appeared in clinical practice: Which technique (Diffusion-Weighted Imaging or 1H-MR Spectroscopy) is more accurate for grading brain tumors in children, or whether both techniques should be used in a combined manner.

Patients and Methods: 100 child with brain tumors were investigated with conventional MRI, DWI, and MRS. The apparent diffusion coefficient (ADC) and spectroscopic metabolites values were retrieved and compared with the tumor grade based on the World Health Organization (WHO) classification of brain tumors.

Results: Average ADC value of the tumors is more accurate than the spectroscopic metabolite values in grading of brain tumors in the children. Average ADC value had high performance in detection of the tumor grade reaching 96.2% with 0.95 x10⁻³ mm²/sec is a cutoff value between the high and low grade by sensitivity 90.9% and specificity 91% [15,20]. On other side the probability of Ch/NAA ratio of the lesion is 86% with 7.4 is a cutoff value between the high- and low-grade tumor by sensitivity 23% and specificity 50%.

Correspondence to: Dr. Mahmoud M.A. Rezk, The Department of Radio-Diagnosis, National Cancer Institute, Cairo University *Conclusion:* Calculated ADC value is more accurate and sensitive than the MRS as non-invasive methods to predict the brain tumor grade in children.

Key Words: Brain Tumors – Pediatric – Diffusion – Weighted Imaging MR – Spectroscopy – ADC – NAA ratio – Tumor grading.

Introduction

PEDIATRIC brain tumors are heterogeneous in cell type. Prognosis depends on tumor grade, stage, and resection extent. Low-grade tumors may require only surgery, while high-grade tumors need adjuvant therapy [1,2]. Conventional MRI delineates tumor location but lacks grading accuracy [3,4]. Biopsy, though definitive, is invasive and prone to sampling error [1].

DWI quantifies cellularity via ADC, while MRS assesses metabolic profiles (e.g., elevated Ch/NAA in high-grade tumors) [5-7]. Prior studies report conflicting results on their standalone versus combined utility [8-10]. This study evaluates their comparative accuracy in pediatrics [11,12].

Conventional MRI helps to characterize the location and extent of these tumors, but it provides limited information regarding tumor type and grade. Consequently, conventional MR imaging falls short as a definitive diagnostic examination; that role is reserved for histopathologic evaluation after biopsy [13-15].

However, the tissue sampling is invasive and has the potential limitations of sampling error.

MR techniques as DWI and MRS are introduced as an non-invasive physiology based tools to provide information about the tumor cellularity by DWI and about the metabolites composition of tumors by MRS thus may help in grading of the tumors. Many investigators studied both techniques either separately and in combined. They report their accuracy in grading of tumors [16-18].

Patients and Methods

Retrospective review of 100 patients with histologically proved brain tumor that were referred to our institution. Totally cystic tumors were excluded from this study. The mean (±SD) age of the patients was 6.08±3.6 years (range from 11 months to 17 years); there were 59 male and 41 female patients. DWI and MRS are part of our institutional protocols, so no additional consent was necessary. Children were examined at initial presentation and before any surgical or adjuvant therapy. In all cases, children were operated upon and tumor specimens were reviewed by an experienced neuropathologist after surgical resection (Table 1).

Methods:

Conventional MR imaging was performed on 1.5T MR units with a protocol that included sagittal noncontract T1-weighted, axial spin-echo T2-weighted, axial fluid-attenuated inversion recovery (FLAIR), as well as postcontrast enhanced axial, coronal, and sagittal T1-weighted images.

DWI was acquired by using b values of 0, 500, and 1000 s/mm² applied in the Z, Y, and X directions. Processing of ADC maps was performed automatically on the MR scanners. The ADC was measured by manually placing regions of interest (ROI) 50–100 mm² in tumor regions on the ADC map. We compared the ADC maps and other MR images carefully and placed the ROI only in the solid tumor components. We excluded cystic, necrotic, and hemorrhagic tumor areas. We chose three random ROIs as centrally as possible within the tumor area and averaged the ADC values. In patients with contrast-enhancing tumors, ROIs were placed at the site of enhancement. In patients with weakly enhancing or non-enhancing tumors, ROIs were chosen after identifying the tumor area as an area of hyperintensity on FLAIR images. Cystic components were differentiated as both areas of hyperintensity on T2-weighted MR images and areas of hypo intensity on FLAIR MR Images. Necrotic components were differentiated on contrast-enhanced T1-weighted images as the no enhancing regions within the enhancing tumor. Hemorrhagic lesions were differentiated on unenhanced

T1-weighted MR images as areas of hyperintensity. Another similar ROI was placed in normal brain tissue and relative ADC was calculated as ADC of lesion / ADC of normal tissue.

MRS technique: All cases were evaluated by single voxel spectroscopic technique using spin- echo sequence (point-resolved spectroscopy [PRESS]) using intermediate TE (144 msec) The voxel was positioned in solid enhanced component on the post GD series, in cases with non enhanced lesion; the region of interest is selected in solid lesion (determined by hypo-intense on T1WI, bright signal on T2WI and FLAIR). In all case, the areas of hemorrhage or necrosis are avoided. Also avoid contamination from the nearby bone or CSF spaces. The voxel size ranged from 1x1x1 cm to 2x2x2 cm. Another similar voxel was positioned on the contra lateral normal appearing brain tissue to obtain a reference spectrum.

Spectroscopic data analysis: The time versus signal intensity was processed to remove residual water signal. Post processing of the spectroscopic data consisted of frequency shift, phase and linear baseline correlation after Fourier transformation. Frequency domain curve was fitted to Gaussian line shape by using soft ware provided by manufacturer to define NAA at 2.02 ppm, Choline (Ch) at 3.02 ppm, cr at 3.01 and lactate at 1.33ppm metabolic values were calculated automatically from the area under the metabolic peak using the standard commercial soft ware program provided by the manufacturer. Peak integral values were normalized to the internal Cr peak. Metabolite ratios of Choline/NAA, NAA/Cho, NAA/Cr, Cho/Cr were calculated.

Histopathologic classification: During the surgery, total resection or multiple biopsy specimens, which minimally measured 2 x 2 x2 cm were obtained from each patient. Specimens were fixed in formalin and submitted for routine hematoxylin-eosin staining in addition to immunohistochemistry for glial fibrillary acidic protein. After tumor classification, the presence of necrosis, astrogliosis, and macrophage infiltration were noted for each tumor.

Tumors were graded by using WHO criteria as WHO grades I-IV, with grades I and II considered as low grade and grades III and IV as high grade tumors. Germ cell tumors are classified as high grade tumors.

Statistical analysis: Analysis of data was done using SPSS (statistical program for social science) program. We used the Chi-square test to compare

Mahmoud M.A. Rezk, et al. 1531

qualitative variables and the Fisher exact probability test when the study group was <5. The correlation coefficient test (r-test) was used to rank different variables against each other either positively or inversely. Sensitivity and specificity were calculated. p-value <0.05 was considered significant and p-value <0.01 was considered highly significant.

Results

A total of 100 pediatric patients with histologically confirmed brain tumors were included. The distribution of tumor pathologies and WHO grades is detailed in Table (1).

Table (1): Pathology distribution and WHO grades.

Pathology	No. of cases (%)	WHO grade	
Desmoplastic infantile	1 (1.0)	(I) Low grade	
astrocytoma			
DNET	2 (2.0)	(I) Low grade	
Pilocytic astrocytoma	17 (17.0)	(I) Low grade	
Subependymal giant cell	2 (2.0)	(I) Low grade	
astrocytoma			
Ganglioglioma	4 (4.0)	(I) Low grade	
Chordoid glioma	1 (1.0)	(II) Low grade	
Pilomyxoid astrocyctoma	2 (2.0)	(II) Low grade	
Ependymoma	4 (4.0)	(II) Low grade	
Fibrillary astrocytoma	10 (10.0)	(II) Low grade	
Anaplastic ependymoma	9 (9.0)	(III) High grade	
Choroid plexus carcinoma	1 (1.0)	(III) High grade	
High grade astrocytoma	1 (1.0)	(III) High grade	
ATRT	3 (3.0)	(IV) High grade	
Glioblastoma	2 (2.0)	(IV) High grade	
Gliosarcoma	1 (1.0)	(IV) High grade	
Medulloblastoma	34 (34.0)	(IV) High grade	
Pineoblastoma	1 (1.0)	(IV) High grade	
PNET	3 (3.0)	(IV) High grade	
Germinoma	2 (2.0)	High grade	
Total	100		

Raw patient data, including sex, age, location, pathology, grade, ADC values Table (2), and spectroscopic metabolites (Ch, NAA, Cr, lactate, ratios), were compiled from the provided Table (3). xlsx (Sheets "ENDED" "and"). Due to the large dataset (200 entries across sheets), key aggregates are used here; full data available in source file. For example, sample entries show lower ADC in high-grade tumors (e.g., medulloblastoma: ADC ~0.6-0.8 x10⁻³ mm²/s) vs low-grade (e.g., pilocytic astrocytoma: ~1.5-1.8).

ADC values demonstrated significant differences between high- and low-grade tumors, as shown in Table (2) (Fig. 1).

Spectroscopic parameters showed correlations with tumor grade, as detailed in Table (3) (Fig. 2).

The ADC value exhibited a higher probability (96.1%) for accurate grading compared to the Ch/NAA ratio (86%). ADC also showed superior sensitivity (90.9%) but slightly lower specificity than Ch/NAA. The cutoff for ADC between high and low-grade tumors was $0.95 \times 10^{-3} \text{ mm}^2/\text{s}$. No grade I tumors were separately analyzed, with focus on low (I-II) (Figs. 3,4) vs high (III-IV) (Fig. 5). The combination of techniques improved differentiation, with ADC at 91.3% accuracy for grade II vs high-grade.

Table (2): Mean, median, and range of absolute and relative ADC values in low- and high-grade tumors.

	Mean ± Std	Median	Range
High Grade: ADC of lesions $x10^{-3}$ mm ² /s	0.71±0.19	0.68	0.4 – 1.2
High Grade: Relative ADC	0.89±0.25	0.84	0.49 – 1.71
Low grade: ADC of lesions $x10^{-3} \text{ mm}^2/\text{s}$	1.508±0.43	1.556	0.6 – 2.9
Low grade: Relative ADC	1.84±0.57	1.91	0.86 - 3.85

Table (3): Significance and correlation of spectroscopic parameters with tumor grade.

	r	Sig.
Grade classification with Ch	0.59	0.00
Grade classification with NNA	-0.10	0.29
Grade classification with Cr	0.36	0.00
Grade classification with Ch / NNA	0.50	0.00
Grade classification with Ch / Cr	0.03	0.71
Grade classification with NNA / Ch	-0.38	0.00
Grade classification with NNA / Cr	-0.25	0.01
Grade classification with NNA / $Ch + Cr$	-0.47	0.00
Grade classification with Lactate	-0.0	0.98

[The long 100-case listing table has been removed as requested]

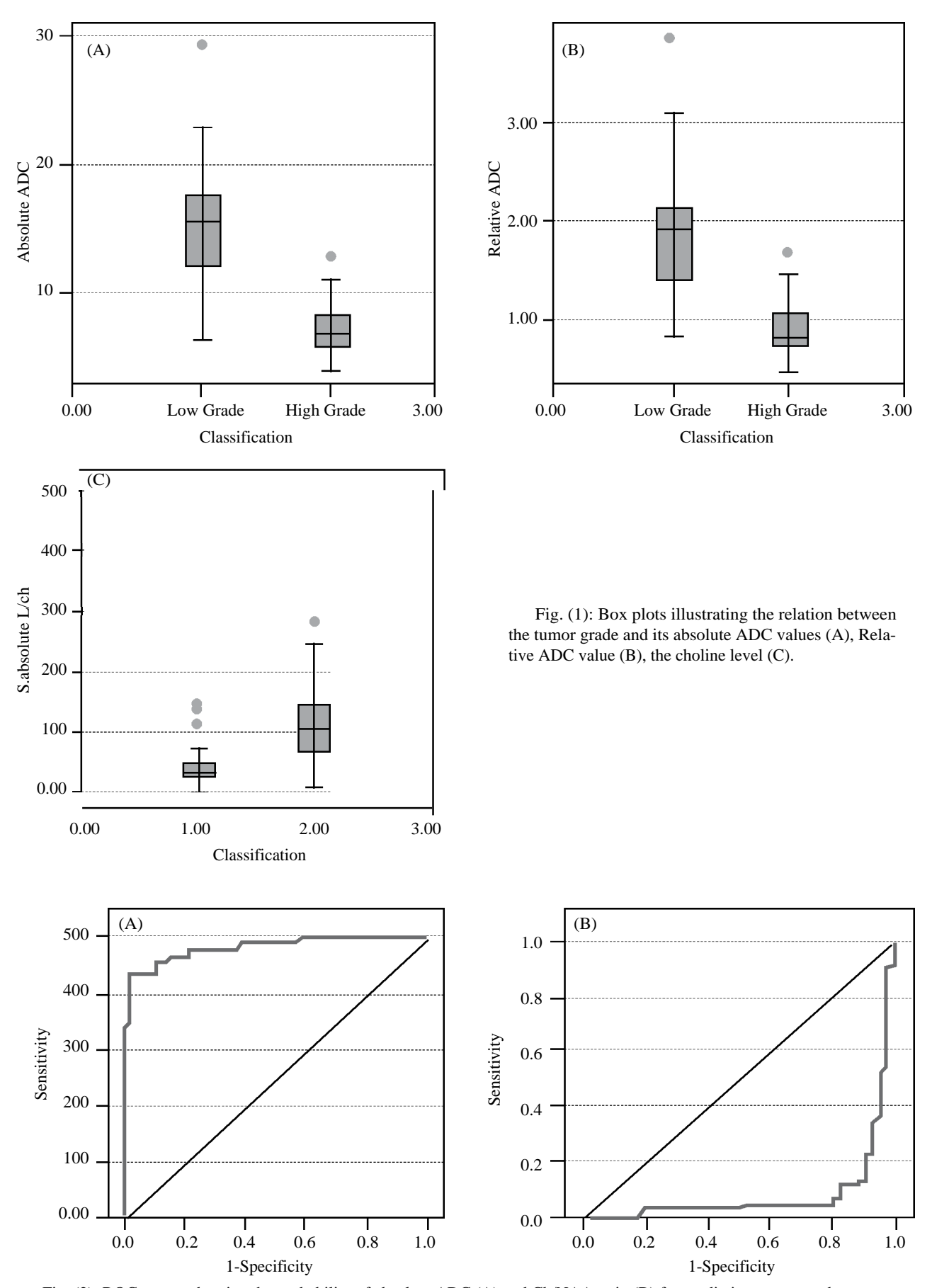


Fig. (2): ROC curves showing the probability of absolute ADC (A) and Ch/NAA ratio (B) for predicting tumor grade.

Mahmoud M.A. Rezk, et al. 1533

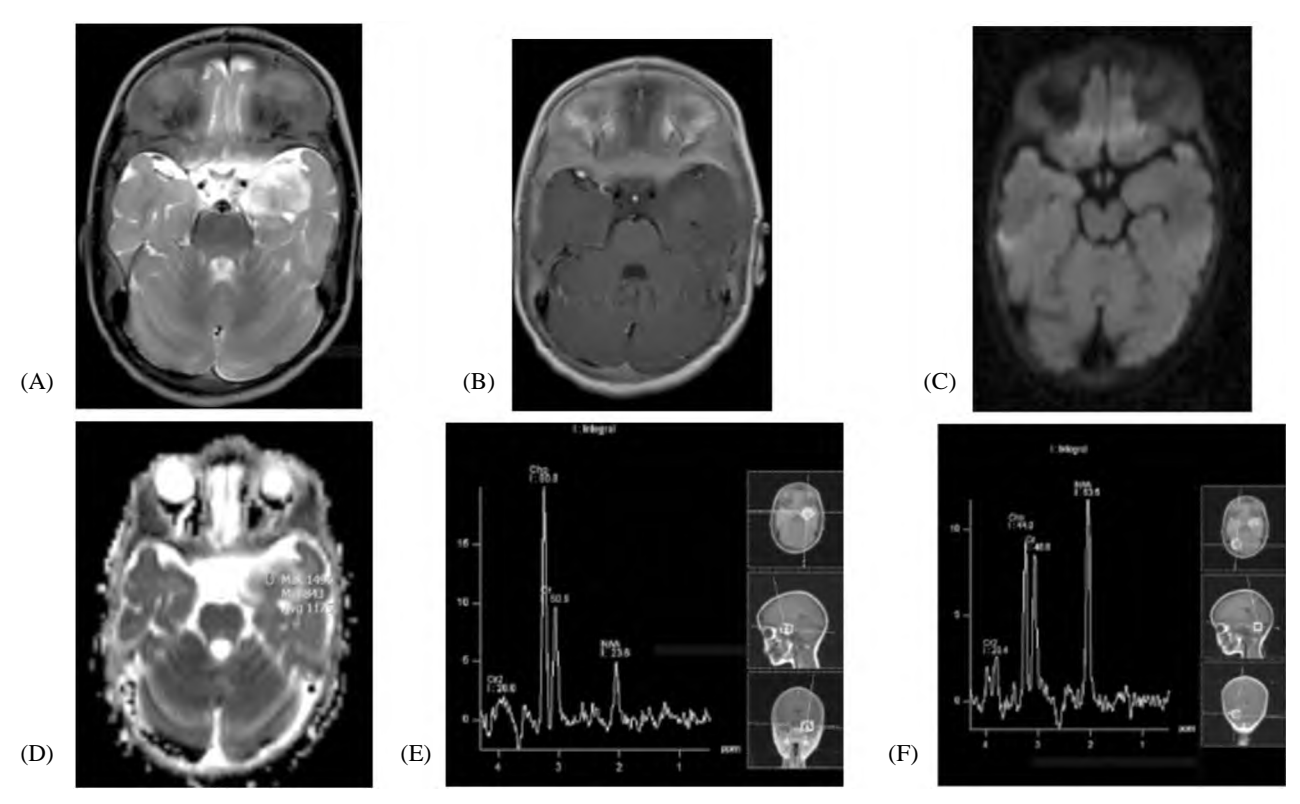


Fig. (3): A 4-year-old girl with epilepsy. (A) Axial T2WI shows a well-defined, irregular intra-axial lesion in the left temporal cortex. (B) Contrast-enhanced T1WI shows faint enhancement, (C) DWI shows isointense signal, (D) ADC map indicates elevated ADC (1.1 x 10⁻³ mm²/s vs. 0.9 x 10⁻³ mm²/s in normal tissue). (E & F) MRS shows increased choline (91 vs. 44), reduced NAA (24 vs. 64), Ch/NAA=3.8, no lactate peak. Pathology: Ganglioglioma, WHO Grade I.

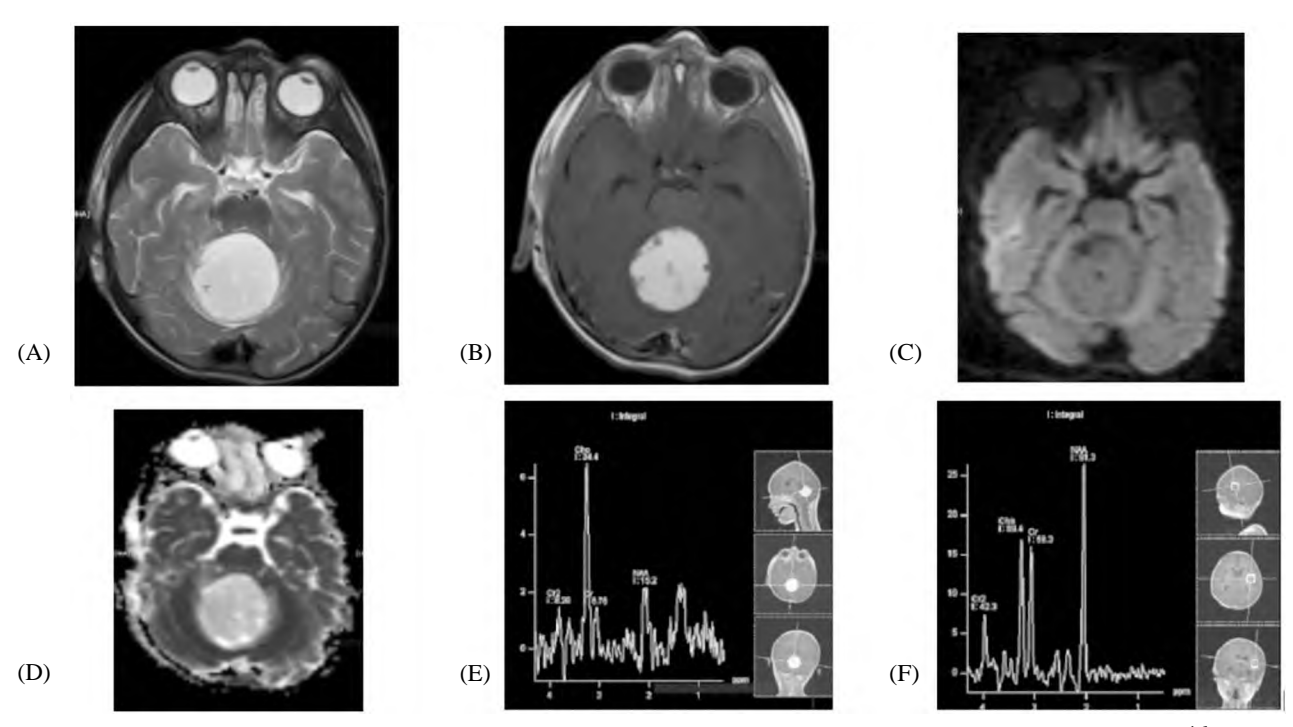


Fig. (4): A 3-year-old with gait disturbance, (A) Axial T2WI shows a midline posterior fossa lesion encroaching on the ^{4th} ventricle. (B) Contrast-enhanced T1WI shows vivid enhancement. (C) DWI shows iso-to hypointense signal, (D) ADC map shows elevated ADC (1.8 x 10⁻³ mm⁻²/s vs. 0.9 x 10⁻³ mm⁻²/s). (E&F) MRS shows reduced choline (34 vs. 69), NAA (15 vs. 91), Ch/NAA=2.2, small lactate peak. Pathology: Diffuse astrocytoma with piloid features, WHO Grade II.

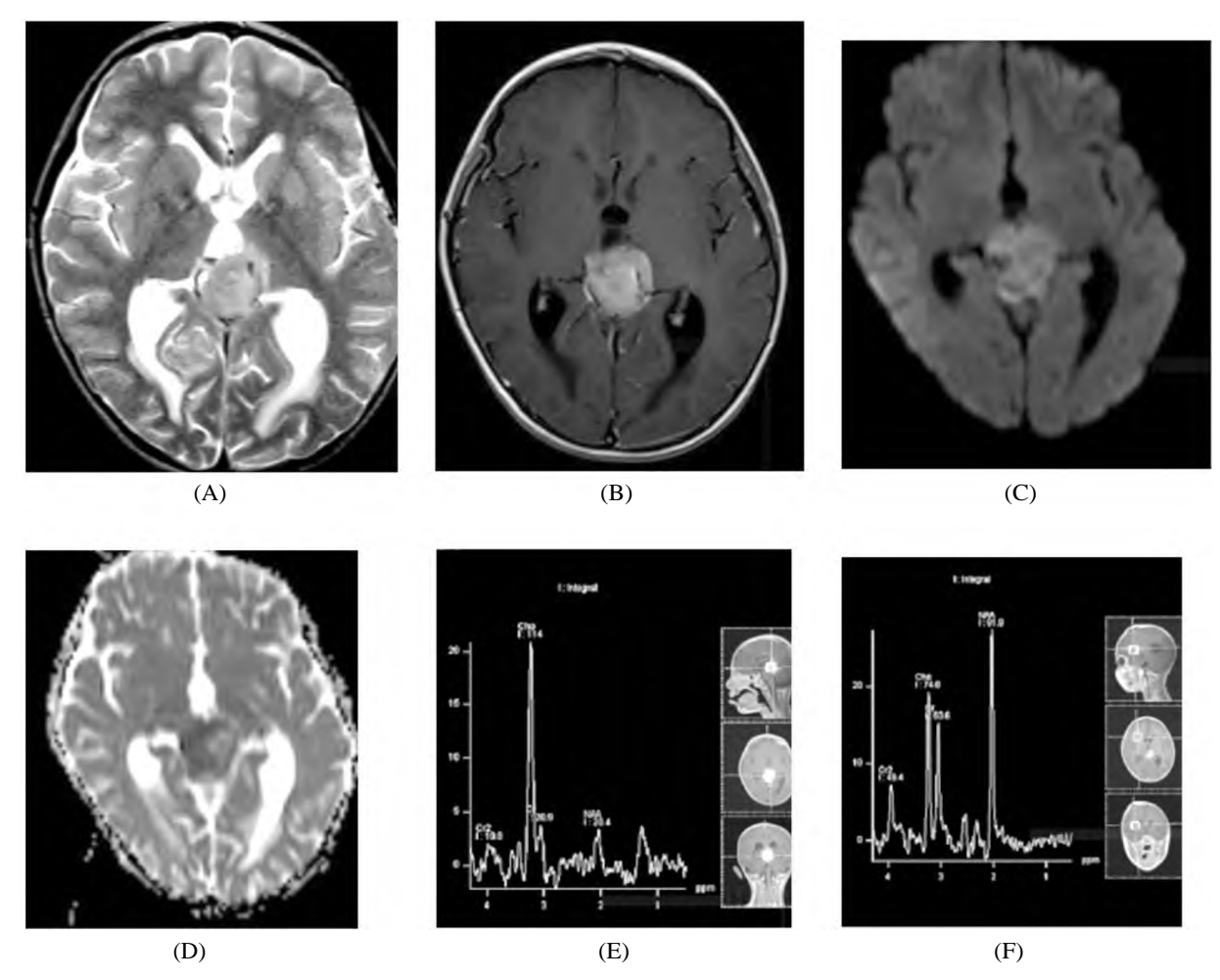


Fig. (5): A 4-year-old female with abnormal eye movement. (A) Axial T2WI shows an isointense pineal region lesion. (B) Contrast-enhanced T1WI shows intense enhancement. (C) DWI shows bright signal. (D) ADC map shows reduced ADC (0.6 x 10^{-3} mm /s vs. 0.8 x 10^{-3} mm /s). (E&F) MRS shows increased choline (114 vs. 74), reduced NAA (20 vs. 92), Ch/NAA=5.5, small lactate peak. Pathology: Pineoblastoma, WHO Grade IV.

Discussion

In this retrospective study of 100 pediatric patients with brain tumors, we compared the utility of DWI-derived ADC values and 1H-MRS metabolite ratios for non-invasive tumor grading, benchmarked against WHO histopathological classification [1]. Our findings indicate that ADC values provide superior accuracy, sensitivity, and predictive probability for distinguishing low-grade (WHO I-II) from high-grade (WHO III-IV) tumors compared to MRS parameters, particularly the Ch/NAA ratio [3,9].

The mean ADC in high-grade tumors $(0.71\pm0.19 \times 10^{-3} \text{ mm}^2/\text{s})$ was significantly lower than in low-grade tumors $(1.508\pm0.43 \times 10^{-3} \text{ mm}^2/\text{s})$ [15,20], reflecting increased cellular density and restricted diffusion in aggressive malignancies. This aligns with established literature, where reduced ADC

correlates with higher tumor cellularity and grade [4,13]. Using a cutoff of $0.95 \times 10^{-3} \text{ mm}^2/\text{s}$, ADC achieved 96.2% probability, 90.9% sensitivity, and 91% specificity, outperforming prior studies that reported ADC sensitivities of 80-85% in adults but highlighting its robustness in pediatrics [3,9].

MRS analysis revealed significant correlations for several metabolites: Elevated Ch (r=0.59, p<0.01) and Ch/NAA (r=0.50, p<0.01) in high-grade tumors, indicative of membrane turnover and neuronal loss, while NAA/Ch showed inverse correlation (r=-0.38, p<0.01) [9]. However, the Ch/NAA ratio's diagnostic probability was lower at 86%, with poor sensitivity (23%) despite moderate specificity (50%), using a cutoff of 7.4 [7,8]. This is consistent with earlier reports where MRS aids characterization but struggles with heterogeneous pediatric tumors [19,20].

When comparing techniques, ADC's higher sensitivity addresses MRS limitations, such as voxel placement errors in heterogeneous tumors and lower resolution for metabolites like lactate (non-significant correlation, r=-0.0) [9,21]. Our results showed ADC probability (96.2%) exceeding Ch/NAA (86%) [9,15], with combined use improving grade II vs high-grade accuracy to 91.3% [6,11]. This supports multiparametric approaches in recent literature, where DWI outperforms MRS in time-constrained pediatric scans [22-24].

Limitations include the retrospective design, potential biopsy-ROI mismatch, and exclusion of totally cystic tumors, which may bias toward solid lesions [24,25]. Single-voxel MRS limits spatial coverage compared to multivoxel methods, and the 1.5T field strength may reduce metabolite resolution [20-25]. Future studies could incorporate advanced sequences like multiparametric MRI or AI for enhanced grading [16,17].

In clinical practice, DWI's short acquisition time (1-2 minutes) makes it preferable for pediatric patients requiring anesthesia, versus MRS (up to 20 minutes) [26,27]. Our recommendation: Prioritize ADC for initial grading, with MRS as adjunct for equivocal cases [28-30].

References

- 1- MCNAMARA C., MANKAD K., THUST S., et al.: 2021 WHO classification of tumors of the central nervous system: A review for the neuroradiologist. Neuroradiology, 64: 1919–1950, 2022.
- 2- Pediatric neuro-oncology: Highlights of the last quarter-century. Neurooncol. Adv., Jun 28; 6 (1): vdae101, 2024.
- 3- ROMANO A., PALIZZI S., ROMANO A., et al.: Diffusion weighted imaging in neuro-oncology: Diagnosis, post-treatment changes, and advanced sequences an updated review. Cancers (Basel), 15: 618, 2023.
- 4- SHINYA OSHIRO, HITOSHI TSUGU, FUMINARI KO-MATSU, et al.: Quantitative assessment of gliomas by proton Magnetic resonance spectroscopy. Anticancer Research, 27: 3757-64, 2007.
- 5- SCHNEIDER J.F., CONFORT-GOUNY S., VIOLA A., et al.: Multiparametric Differentiation of Posterior Fossa Tumors in Children Using Diffusion-Weighted Imaging and Short Echo-Time 1H-MR Spectroscopy J. Magn. Reson. Imaging, 26: 1390–98, 2007.
- 6- PANIGRAHY, KRIEGER, GONZALEZ-GOMEZ I., et al.: Quantitative Short Echo Time 1H-MR Spectroscopy of Untreated Pediatric Brain Tumors: Preoperative Diagnosis

- and Characterization. AJNR Am. J. Neuroradiol. Mar., 27: 560-72, 2006.
- 7- LEACH M.O.: Magnetic resonance spectroscopy (MRS) in the investigation of cancer at The Royal Marsden Hospital and The Institute of Cancer Research. Phys. Med. Biol., 51: R61–R82, 2006.
- 8- WU H-W., WU C-H., LIN S-C., et al.: MRI features of pediatric atypical teratoid rhabdoid tumors and medullo-blastomas of the posterior fossa. Cancer Med., 12: 10449–461, 2023.
- 9- ROLLIN, GUYOTAT, STREICHENBERGER, et al.: Clinical relevance of diffusion and perfusion magnetic imaging in assessing intra-axial brain tumors. Neuroradiology, 48: 150–9, 2006.
- 10- ZHANG K., LI C., LIU Y., et al.: Evaluation of invasiveness of astrocytoma using 1H-magnetic resonance spectroscopy: Correlation with expression of matrix metalloproteinase-2. Neuroradiology, 49: 913–9, 2007.
- 11- LAW M., YANG S., WANG H., et al.: Glioma grading: Sensitivity, specificity, and predictive values of perfusion MR imaging and proton MR spectroscopic imaging compared with conventional MR imaging. Am. J. Neuroradiol., 24: 1989–98, 2003.
- 12- The Role of Multiparametric MRI in the Non-Invasive Diagnosis of Malignancy Degree of Pediatric Intracranial Tumors: A Single-Center Study. Diagnostics (Basel), Dec. 9; 13 (24): 3617, 2023.
- 13- MOLLER-HARTMANN W., HERMINGHAUS S., KRI-NGS T., et al.: Clinical application of proton magnetic resonance spectroscopy in the diagnosis of intracranial mass lesions. Neuroradiology, 44: 371-81, 2002.
- 14- LEE E.J., LEE S.K., AGID R., et al.: Preoperative grading of presumptive low-grade astrocytomas on MR imaging: Diagnostic value of minimum apparent diffusion coefficient. Am. J. Neuroradiol., 29: 1872–7, 2008.
- 15- MURAKAMI R., HIRAI T., SUGAHARA T., et al.: Grading astrocytic tumors by using apparent diffusion coefficient parameters: Superiority of a one-versus two parameters pilot method. Radiology, 251: 838–45, 2009.
- 16- Radiomics and Artificial Intelligence Applications in Pediatric Brain Tumors: A Review. Cancers (Basel), Jul 9; 16 (14): 2495, 2024.
- 17- Insights Into Histological Grading and IDH Classification.
 J. Magn Reson Imaging. May 15, 2024.
- 18- LAM W.W., POON W.S., METREWELI C., et al.: Diffusion MR imaging in glioma: Does it have any role in the preoperative determination of grading of glioma? Clin. Radiol., 57: 219–25, 2002.
- 19- ARVINDA H.R., KESAVADAS C., SARMA P.S., et al.: Gliomas grading: Sensitivity, specificity, positive and neg-

- ative predictive values of diffusion and perfusion imaging. J. Neurooncol., 94: 87–96, 2009.
- 20- YAMASAKI F., KURISU K., SATOH K., et al.: Apparent diffusion coefficient of human brain tumors at MR imaging. Radiology, 235: 985–91, 2005.
- Advanced Neuroimaging Approaches to Pediatric Brain Tumors. Curr. Neurol. Neurosci. Rep., Aug. 23 (8): 375-390, 2023.
- 22- Imaging of pediatric brain tumors: A COG Diagnostic Imaging Committee/SPR Oncology Committee/ASPNR White Paper. Pediatr Blood Cancer, Jun. 70 (Suppl 4): e30147, 2023.
- 23- Characterization of paediatric brain tumours by their MRS metabolite profiles. NMR Biomed, Feb 20: e5125, 2024.
- 24- Diffusion-weighted imaging in pediatric central nervous system infections. Neuroradiology, Dec. 65 (12): 1701-1711, 2023.
- 25- Basics for Pediatric Brain Tumor Imaging: Techniques and Protocols. Semin Ultrasound CT MR, Apr. 45 (2): 127-137, 2024.

- 26- Incidental brain tumor findings in children: Prevalence, natural history, and recommendation. Neuroradiology, Jul. 29, 2024.
- 27- GOEBELL E., PAUSTENBACH S., VAETERLEIN O., et al.: Low-grade and anaplastic gliomas: Differences in architecture evaluated with diffusion-tensor MR imaging. Radiology, 239: 217–22, 2006.
- 28- ANDRÉS SERVER, BETTINA KULLE, YSTEIN, GAD-MAR, et al.: Measurements of diagnostic examination performance using quantitative apparent diffusion coefficient and proton MR spectroscopic imaging in the preoperative evaluation of tumor grade in cerebral gliomas. European Journal of Radiology, 80: 462–70, 2011.
- 29- SUGAHARA T., KOROGI Y., KOCHI M., et al.: Usefulness of diffusion-weighted MRI with echo-planar technique in the evaluation of cellularity in gliomas. J. Magn Reson Imaging, 9: 53–60, 1999.
- 30- WEBER M.A., ZOUBAA S., SCHLIETER M., et al.: Diagnostic performance of spectroscopic and perfusion MRI for distinction of brain tumors. Neurology, 66: 1899–906, 2006.

تصنيف أورام الدماغ لدى الأطفال : دراسة مقارنة بين التصوير بالانتشار الموزون والطيف النووى المغناطيسي

الخلفية والفرض: التشخيص الأولى الدقيق وتصنيف أورام الدماغ يؤثران بشكل كبير على خيارات العلاج، التكهن بالمال، وجودة الحياة الناجين [٣]. يوفر التصوير بالرنين المغناطيسى التقليدي دقة محدودة في تصنيف الأورام، حيث يُعد الفحص النسيجي بعد الخزعة المعيار الذهبي [٣]. يُستخدم التصوير بالانتشار الموزون (DWI) والطيف النووي (MRS) كأدوات غير جراحية لتصنيف الأورام [٥,٠]. تهدف هذه الدراسة إلى مقارنة فعالية هاتين التقنيتين.

الطرق: خضع ١٠٠ طفل مصاب بأورام دماغية التصوير بالرنين المغناطيسى التقليدي، DWI ، و MRS. تم تحليل قيم معامل الانتشار الظاهري (ADC) ونسب المستقلبات الطيفية ومقارنتها مع درجات الأورام حسب تصنيف منظمة الصحة العالمية [٣].

النتائج: أظهرت قيم ADC دقة أعلى من نسب المستقلبات الطيفية فى تصنيف أورام الدماغ لدى الأطفال، مع احتمالية ٩٦,٢٪ لتحديد الدرجة بدقة عند قيمة حد ٩٠,٠٠ تا ٠٠ ٣ مم٢/ثانية (حساسية ٩٠,٠٠٪، خصوصية ٩٠٪) [١٥،٢٠]. فى المقابل، سجلت نسبة احتمالية ٨٦٪ عند قيمة حد ٧,٤ (حساسية ٢٣٪، خصوصية ٥٠٪) [٩،١٢].

الخاتة: قيم ADC أكثر دقة وحساسية من MRS كطريقة غير جراحية لتوقع درجة الورم لدى الأطفال، مما يدعم استخدام DWI كخيار أولى في الممارسة [٦،١٧].